Surface-Activated Nanoparticles for Controlled Light-Responsiveness

Sungsook Ahn, Sung Yong Jung, and Sang Joon Lee**

Most of the optical properties of nanoparticles (NPs) depend on a nonadditive effect, where there is a maximum (or optimum) value at a specific distance from the NP surface (proximity length). However, knowledge on the relation between the specific surface layer and light responsiveness of NPs is limited. In this study, surface properties of NPs are modulated by electron beam (e-beam) treatment together with ionic control of the NP surface and dispersing media. The surface modification in terms of the proximity length is found to be critical to the selective enhancement of light absorbance in the ultraviolet-visible (UV-vis) and terahertz (THz) regions. In particular, the non-temporarily electron-activated NPs absorb short wavelength UV-vis light, rendering them particulary advantageous for solar energy use. The control over the physical properties of general light-responsive NPs is a new approach to designing solar-energy-based technologies.

At present, only limited materials are available for solar energy utilization. Therefore, expansion of the availability of photoactive materials for light energy use is important, for which effective metamaterial design can be a solution. Materials of preferably high absorbance in the short wavelength UV-vis spectrum are advantageous for solar energy utilization, because the solar spectrum reaching the earth is concentrated in this region.[1] To control the light-responsiveness of nanostructured materials, size and shape effects have been broadly studied.[2] In addition, optical properties of nanoparticles (NPs) are dominated by their surface properties which become more important as the NP size decreases. At frequencies of hundreds of gigahertz and lower, the electron is the principal workhorse, whereas in the infrared (IR) to ultraviolet-visible (UV-vis) region, the photon is the fundamental particle. Between these two regimes, in the "terahertz gap", few natural materials are responsive.[3] However, by the electron behavior of designed metal surfaces such as gold or copper, the electromagnetic properties are generated within this gap.[4] By designing effective metamaterials,[5] the absorption yield in microwave,[6] terahertz (THz),[7] and infrared[8] frequencies are enhanced. Moreover, by utilizing surface plasmon resonance in metallic nanostructures,[9] the responsiveness in the UV-vis spectrum can be modified.

Some nanometer-scale properties are additive and others are cooperative. Many optoelectronic properties of metal NPs are cooperative, thus the maximum (or optimum) values are determined at a certain critical depth, λ (proximity length), by the relation,[10]

$$I(x) = I_\infty - (I_\infty - I_r)e^{-(x-r)/\lambda} \quad (1)$$

where x is the distance from the particle surface, r is the physical size of the particle, I_r is the molecular value ($x = r$), and I_∞ is the bulk value per unit surface area ($x = \infty$). Therefore, a bulk intrinsic property, $I(x)/I_\infty$ can be evaluated according to the ratio of NP size to proximity length, r/λ. For one of the optoelectronic properties, conductivity, the λ is inversely proportional to the square root of the frequency.[11] Colloidal quantum dots and NPs are dispersed and utilized in the solution. **Figure 1**A illustrates typical layers around a single particle dispersed in a solvent: the surface charge of a particle (Layer I), the Stern layer (Layer II), and the diffuse layer (Layer IV).[12] In the middle of the diffuse layer, the zeta (ζ)-potential is defined at a specific distance from the particle surface (Debye screening length, Layer III).[13] The ζ-potential is determined by the electrophoretic mobility ($m^2\ V^{-1}\ s^{-1}$) using the Smoluchowski relation when the dispersing medium is water. The hydrodynamic size (D_H) of a particle in the medium is evaluated by the Stokes–Einstein relation by the weight average diffusion coefficient of a particle (D, $m^2\ s^{-1}$).

The stability of the dispersed particles is controlled via particle interaction, changes in pH of the media, ionic strength, type of electrolytes, etc.[14] The surface charge of the particles is controlled by surface ionization and adsorption/dissolution of the ions in the media.[15] Increases in the electrostatic double layer thickness and/or ζ-potential result in increased electrostatic forces among the particles.[16] Considering that the mean-square distance ($<L>^2$) is proportional to the time (t) related with the diffusion coefficient (D) ($<L>^2 \propto Dt$), NP movement is much faster than that of microparticle with units of seconds as

S. Ahn, S. Y. Jung, S. J. Lee
Department of Mechanical Engineering
Pohang University of Science and Technology
Pohang, 790-784, South Korea
E-mail: sungosokahn@postech.ac.kr;
sjlee@postech.ac.kr
S. J. Lee
Center for Biofluid and Biomimic Research
Pohang University of Science and Technology
Pohang, 790-784, South Korea
S. J. Lee
Division of Integrative Biosciences and Biotechnology
Pohang University of Science and Technology
Pohang, 790-784, South Korea

DOI: 10.1002/adfm.201202501

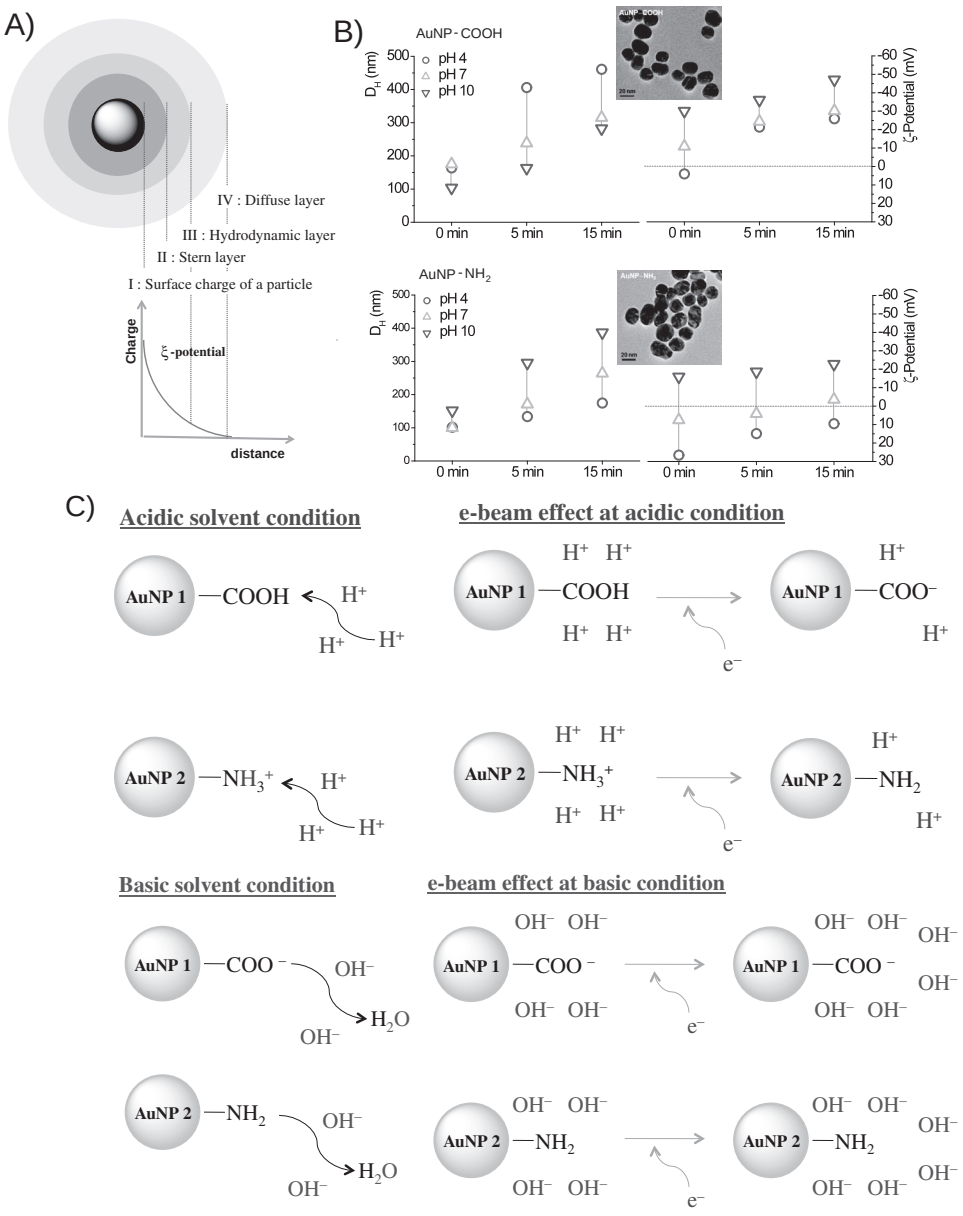

Figure 1. A) Layers around a charged particle. Layer I: the surface charge of a particle is determined. Layer II: stern layer where oppositely charged ions from the particle surface form a layer. Layer III: the ζ potential is determined in the middle of the diffuse layer, where D_H is determined. Layer IV: an electrostatic field is formed from the strong particle surface to the end of the diffuse layer. B) D_H and ζ potential of the AuNP-COOH (upper) and AuNP-NH_2 (lower) systems after e-beam exposure for 0, 5, and 15 min. The insets are the TEM images of each AuNP. C) Surface-modified gold nanoparticles (AuNPs) reacting in acidic and basic conditions. In acidic conditions, H^+ is provided by the environment, whereas in basic conditions, H^+ is removed from the AuNP surface. Electron beam effects on the anionic and cationic AuNPs in pH-controlled conditions. The provided electrons are expected to neutralize the positive ions in acidic condition and promote negative ions in basic conditions.

opposed to years. The agglomeration and stability of dispersed particles are determined by the equilibrium between attractive van der Waals forces and electrostatic repulsive forces.[17] Since the van der Waals adhesion or binding energies increases with increased particle size,[14] the physical properties of NP are less susceptible to the particle aggregation than microparticles. Therefore, NPs are much faster in movement and less aggregated than microparticles, for which the surface properties dominant.

In this study, cationic and anionic gold NPs (AuNPs) of a fixed size (average diameter of 20 nm) were suspended in pH-controlled aqueous solutions, followed by electron-beam (e-beam) treatment to modulate the surface properties. Once the Stern layer is saturated by ions provided from the environment, the excess ions contribute to the diffuse layer, affecting the ζ-potential of the NPs. The effects of acidic and basic solvent on the surface-modified AuNPs are illustrated in Figure 1C. Depending on the introduced functional groups on the AuNP,

absolute isoelectric point varies. Nonetheless, the qualitative ionization tendency of an carboxylic acid- and amine-functional groups on AuNP surface follows a general trend. When anionic AuNP is dispersed in an acidic solvent from which H^+ is provided, the neutralized AuNP–COOH is preferable to the charged AuNP–COO^-. Conversely, in basic solvents, charged AuNP–COO^- becomes advantageous. Similarly, for the cationic AuNP, the charged AuNP–NH_3^+ is abundant in acidic solvents, whereas the noncharged AuNP–NH_2 is preferable in basic solvent.[18]

In Figure 1B, the variations in D_H and ζ-potential are investigated as a function of pH and e-beam exposure time. For each point in the graph, 40 runs were performed for one measurement and three measurements were averaged within a ±5% deviation. For clear comparison, the error ranges are not shown in the graph. D_H and ζ-potential vary according to the pH, however overall variation is more significant with the e-beam exposure up to 15 min. The D_H can be increased by the aggregation of neutralized AuNPs, but the increase in both D_H and ζ-potential indicates the increase in the electrostatic layer on an AuNP. The isoelectric point where the ζ-potential becomes zero, is marked by the horizontal dotted line on the right graph. The isoelectric point approaches at around pH 4 for AuNP–COOH (the pK_a of acetic acid is 4.76).[19]. Meanwhile, that of AuNP–NH_2 is slightly higher than pH 7 (pK_a of 6-thioguanine is 8.26).[20] The ζ-potential increases in the negative direction with increased pH, allowing negatively charged particles to repel each other. However, as observed with both AuNP–COOH (from pH 4 to 7) and AuNP–NH_2 (from pH 7 to 10) without e-beam treatment (at 0 min), the increase in electrostatic layer is observed.

The suggested e-beam effects on the surface-modified NPs are illustrated in Figure 1C. In an H^+ abundant environment (under acidic conditions), the provided e-beam reduces the H^+ concentration of the medium. Under this condition, ionized AuNP–COO^- becomes more dominant than neutral AuNP–COOH. In an OH^- abundant environment (at basic condition), the provided e-beam contributes to more ionized AuNP–COO^- in addition to increased OH^- concentration of the medium. The application of e-beam in the AuNP–NH_3^+ system in an H^+ abundant environment contribute to increase in neutral AuNP–NH_2 as well as decrease in H^+ in the medium. Inversely, under basic conditions, neural AuNP–NH_2 becomes predominant by e-beam application with increased OH^- concentration in the medium. The change in electrostatic double layer is sensitive to the media condition,[21] and the e-beam introduction modifies the surface of the primary particle on which radical reaction can occur.

By the e-beam exposure of the designed AuNPs for 5 and 15 min (Supporting Information), both the D_H and ζ-potential of AuNP–COOH (Figure 1B, upper) and AuNP–NH_2 (Figure 1B, lower) significantly increase. The e-beam treatment can effectively increase the surface charge of the particle (Layer I), followed by the increase in the electrostatic double layer (Layer II) and thus D_H. The ζ-potential of the samples shifts to the negative direction by the exposure to the e-beam, therefore, the e-beam effectively provides electrons to the AuNP-dispersed solutions. In addition, D_H increases proportionally with the exposure time, for both cationic and anionic AuNPs. The observed result indicated that the e-beam treatment systematically modifies the surface properties of charged NPs in ionic solutions, increasing the thickness of the electrostatic layer.

Considering the radius R of a spherical NP and proximity length λ, Equation (1) is rewritten as,

$$I(x)/I_\infty = 3(R/r)\{1-(I_r/I_\infty)-1\}\exp[-\{(R/r)-1](r/\lambda)\}] \quad (2)$$

where R and r are replaced experimentally by D_H and the average core size of the AuNPs (20 nm), respectively (Supporting

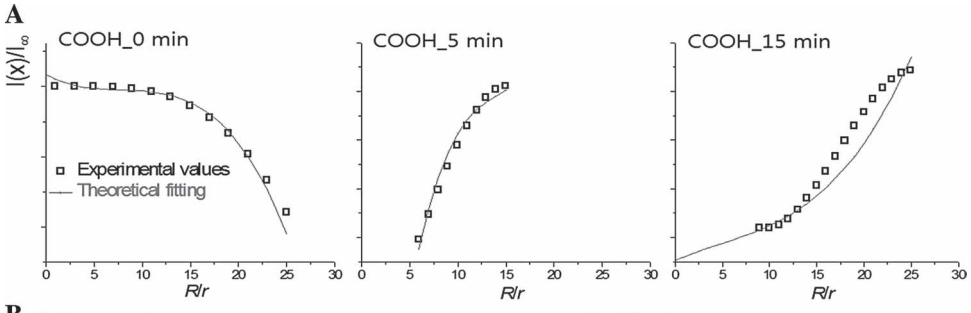

B

AuNP surface	e-beam exposure (min)	I_r/I_∞	r/λ	Deviation* (%)	κ_1§	κ_2¥
–COOH	0	10	10	9	5	-30
	5	0.01	0.01	7	-2.5	1.2
	15	0.001	0.001	5	-1.5	0.5
$–NH_2$	0	0.01	10	8	140	-10
	5	0.001	1	5	0.5	-4
	15	0	0.1	6	-4	1

$$^*\text{Deviation} = \frac{|\{(\text{experimental value}) - [\kappa_1(\text{theoretical value}) + \kappa_2]\}|}{|\{(\text{experimental value}) + [\kappa_1(\text{theoretical value}) + \kappa_2]\}|}$$

§,¥ κ_1 and κ_2 are correction constants (Supporting Information)

Figure 2. A) Equation (1) fitted to the experimental results to the AuNP–COOH and AuNP–NH_2 system of 0, 5, and 15 min e-beam exposure. B) Fitting parameters of the results in (A).

Information). The bulk intrinsic property, $I(x)/I_\infty$ is then plotted against the normalized size R/r by the controlled values of I_r/I_∞ and r/λ. The simulated results are available in Supporting Information Figure S2. The bulk intrinsic property $I(x)/I_\infty$ against the normalized size R/r are dynamically changed by the changing the proximity length λ (r/λ) (Supporting Information Figure S2A). Significant decrease in λ (thus increase in r/λ) leads to the maximum $I(x)/I_\infty$ value close to the point of $R = r$. The variation of $I(x)/I_\infty$ with the relative size, R/r, is also plotted according to the designated I_r/I_∞ (Supporting Information Figure S2B). The increase in I_r/I_∞ significantly affects the graph shape, but the change in r/λ has a relatively small effect in the given range. The experimentally obtained values are evaluated by theoretical fitting in **Figure 2**A. The fitting parameters for each e-beam-exposed sample are summarized in Figure 2B. The fitting results are not differentiated by the different pH conditions but only by the e-beam exposure. With increased e-beam dose by the increased exposure time, I_r/I_∞ and r/λ significantly decrease. The decrease in I_r/I_∞ close to the unit means that the physical property at a specific distance x from the NP surface becomes close to the bulk value. The significant increase in λ explains that the surface layer demonstrating a specific physical property (here, ζ-potential) becomes prominently thicker by e-beam introduction.

To investigate the light-responsiveness of the designed AuNPs, the fs-THz and UV-vis spectra are displayed in **Figure 3**. Frequency-dependent fs-THz absorbance of the AuNPs are plotted to investigate AuNP activation in terms of photoconductivity (Supporting Information) which is proportional to the transmission at the THz wavelength.[22] Without e-beam exposure (0 min), the pH-controlled environment generates only slight difference in absorbance in THz spectrum (Figure 3A,B, left graphs). This finding implies that only the change in pH is not crucial to the light-responsiveness control of NPs. However, exposure to the e-beam for both AuNP–COOH and AuNP–NH_2 significantly increases the absorbance especially at pH 7 condition and in deionized-water condition, particulary at higher wavelengths. This indicates that e-beam introduction significantly decreases the photoconductivity of the NPs dispersed in neutral solvents. Regardless of the exposure time, once there is a change in light-responsiveness of the NPs the absorbance pattern is similar, reflecting that the physical property change by e-beam is qualitative and non-temporary.

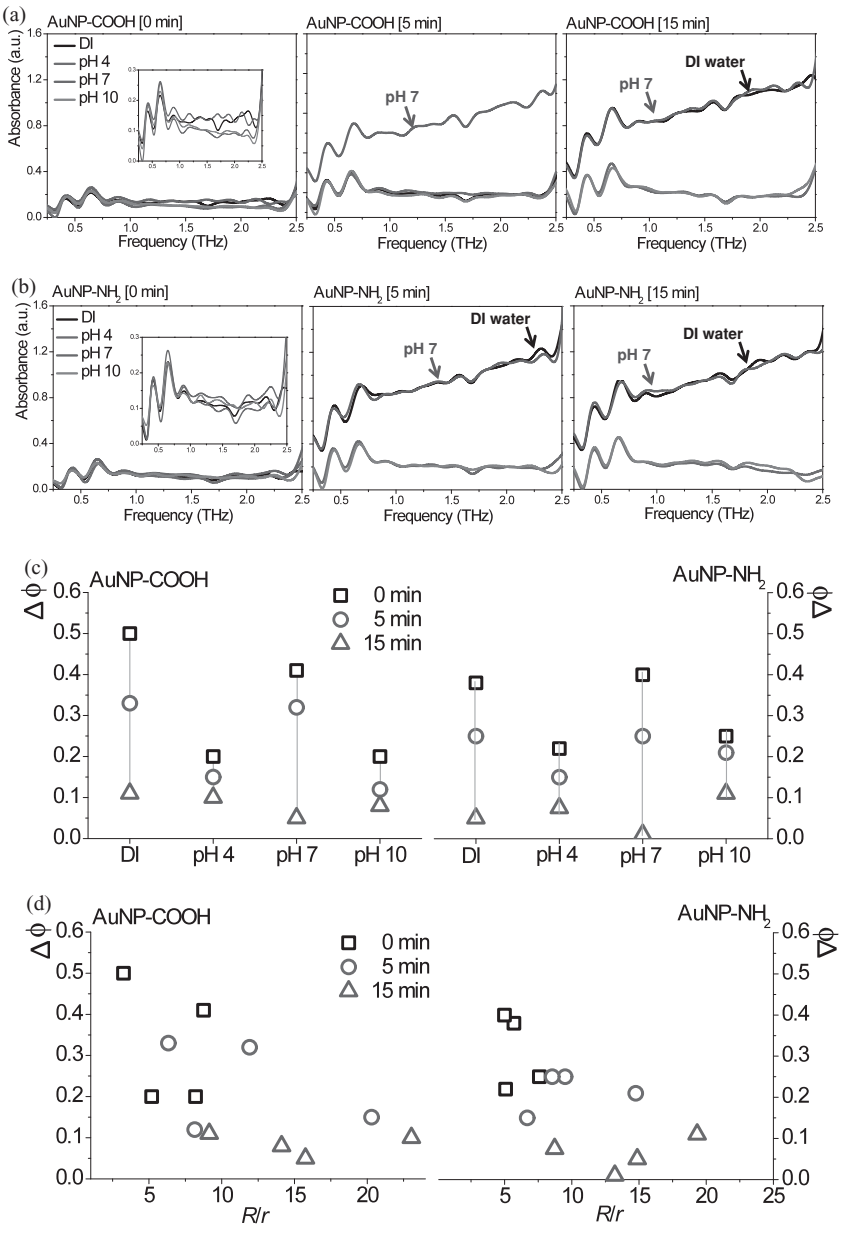

Figure 3. fs-THz spectrum of the AuNP–COOH and AuNP–NH_2 systems after e-beam exposure for 0, 5, and 15 min. Frequency-dependent fs-THz absorbance of the A) AuNP-COOH and B) AuNP-NH_2. Phase changes ($\Delta\varphi$) at 1 THz according to the C) solvent conditions and D) relative particle size (R/r).

The variations in the phase change $\Delta\varphi$ at 1 THz are displayed according to the solvent condition (Figure 3C) and normalized particle size (R/r) (Figure 3D). R and r are experimentally replaced by the D_H and the physical size of the AuNP (20 nm), respectively. The frequency-dependent data provide useful information on the conduction mechanism.[23]. High $\Delta\varphi$ implies high excitation and ionization as well as effective absorbance of THz radiation of NPs, while low $\Delta\varphi$ implies the opposite. Even under different solvent conditions, long e-beam exposure generates low $\Delta\varphi$, reflecting less effective excitonic states (Figure 3C) in addition to the increase in normalized particle size (R/r) (Figure 3D). However, at the same e-beam exposure time, the decrease in $\Delta\varphi$ is not directly proportional to the increase in the normalized particle size (R/r). In terms of solvent, solution of pH 4 and 10 deactivate the

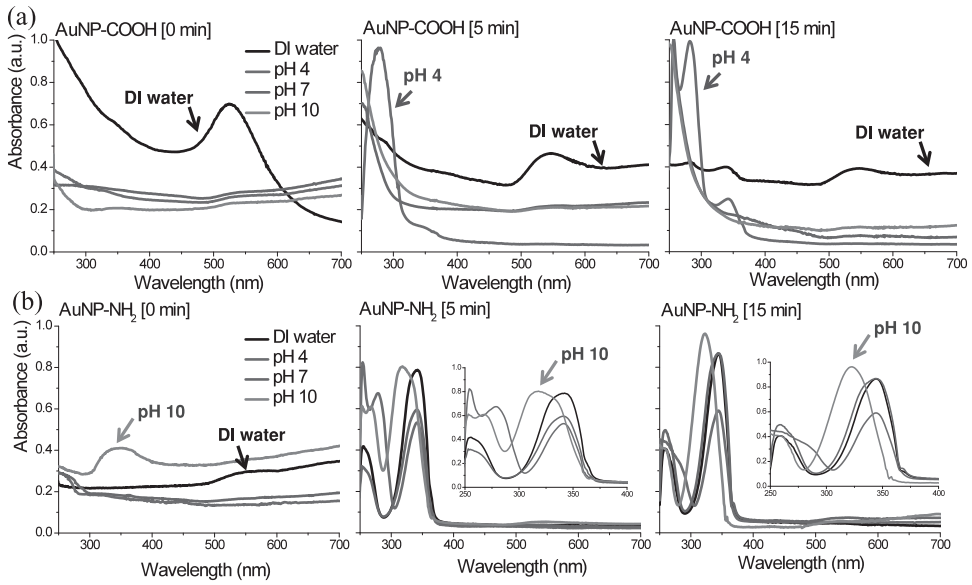

Figure 4. UV-vis spectra of the A) AuNP–COOH and B) AuNP–NH_2 systems after e-beam exposure for 0, 5, and 15 min.

ionization of the NPs, indicated by the low $\Delta\varphi$ values without (0 min) or short-time e-beam introduction (5 min). However, the degree of decrease in $\Delta\varphi$ according to the e-beam exposure is significant in deionized water and in pH 7 solvent, indicating delocalized and non-conductive NP surface formation. The isoelectric points of the designed AuNPs vary; low pH for AuNP–COOH and neutral pH for AuNP–NH_2 (Figure 1B). Nonetheless, both cationic and anionic AuNPs in deionized water and pH 7 solvent become more sensitive to the THz wavelength light than those under other solvent conditions. This result highlights the importance of the medium for the energy activation of NPs. Different from the pH-only control, the introduced e-beam fundamentally activates the NPs under the specific solvent conditions.

The designed AuNP–COOH and AuNP–NH_2 exhibit characteristic optical behavior in the UV-vis region, as shown in **Figure 4**. In the pH-controlled ionic solutions, the characteristic absorbance of AuNPs at around 540 nm significantly decreases. However, e-beam introduction effectively activates the UV-vis absorbance of the AuNPs in the pH-controlled solutions, especially at shorter wavelength regions. The change in UV-vis absorbance by e-beam is non-temporary and qualitative, thus, once there is a change in the absorbance pattern, it is similar regardless of the e-beam exposure time. The characteristic peaks of AuNP–COOH become prominent at pH 4, where the neutral AuNP–COOH form is more preferable than the ionized AuNP–COO^- form. On the other hand, all the AuNP–NH_2 systems are significantly activated by e-beams to enhance the absorbance in the UV-vis region. In particular, the absorbance peak of AuNP–NH_2 shifts to a shorter wavelength region at high pH, where AuNP–NH_2 is more favorable than AuNP–NH_3^+. The e-beam introduction to the AuNP-dispersed solutions promotes the absorbance in the UV-vis spectrum with high intensity at short wavelengths. The neutralized AuNPs by the medium are more effective for the absorbance at short wavelnegth UV-vis spectrum.

In summary, the physical properties of light-responsive NPs are modulated by surface activation. Charged NPs dispersed in ion-controlled solutions differentially respond to a broad light spectrum. Introduction of the e-beam fundamentally modifies the physical properties of the activated NPs in terms of proximity length (λ), which significantly promotes the light-responsiveness in the UV-vis and THz regions. Surface-activated NPs can be further designed with many versatile systems and broadly applied to more effective light energy utilization.

Supporting Information

Supporting Information is available from the Wiley Online Library or from the author.

Acknowledgements

This study was supported by a grant from the National Research Foundation of Korea (NRF) funded by the Korean government Ministry of Education, Science and Technology (MEST) (grant no. 2011-0018947), and jointly supported by the Creative Research Initiatives (Diagnosis of Biofluid Flow Phenomena and Biomimic Research) of MEST, National Science Foundation (NSF) of Korea (grant no. R31-2008-000-10105-0). The authors are grateful to the staff of the Pohang Accelerator Laboratory (Pohang, Korea) for their valuable help in experiments performed using fs-THz spectroscopy and the Pohang Neutron Facility Electron linac (electron beam) beamlines.

Received: August 31, 2012
Published online: November 23, 2012

[1] L. Taiz, E. Zeiger, *Plant Physiology*, Sinauer Associate, Inc., Sunderland **2010**.
[2] T. V. Teperik, F. J. García de Abajo, A. G. Borisov, M. Abdelsalam, P. N. Bartlett, Y. Sugawara, J. J. Baumberg, *Nat. Photonics* **2008**, *2*, 299–301.

[3] G. P. Williams, *Rep. Prog. Phys.* **2006**, *69*, 301–326.
[4] T. J. Yen, W. J. Padilla, N. Fang, D. C. Vier, D. R. Smith, J. B. Pendry, D. N. Basov, X. Zhang, *Science* **2004**, *303*, 1494–1496.
[5] Z. Said, A. Sihvola, A. P. Vinogradov, *Metamaterials and Plasmonics: Fundamentals, Modelling, Applications*, Springer-Verlag, New York **2008**.
[6] N. I. Landy, S. Sajuyigbe, J. J. Mock, D. R. Smith, W. J. Padilla, *Phys. Rev. Lett.* **2008**, *100*, 207402.
[7] H. Tao, N. I. Landy, C. M. Bingham, X. Zhang, R. D. Averitt, W. J. Padilla, *Opt. Express* **2008**, *16*, 7181–7188.
[8] X. L. Liu, T. Starr, A. F. Starr, W. J. Padilla, *Phys. Rev. Lett.* **2010**, *104*, 207403.
[9] S. M. Nie, S. R. Emery, *Science* **1997**, *275*, 1102–1106.
[10] I. V. Antonets, L. N. Kotov, S. V. Nekipelov, E. N. Karpushov, *Tech. Phys.* **2004**, *49*, 1496–1500.
[11] D. Srivastava, M. Menon, K. Cho, *Phys. Rev. B* **2001**, *6319*, 195413.
[12] I. D. Morrison, S. Ross, *Colloidal Dispersions: Suspensions, Emulsions, and Foams*, Wiley-Interscience, New York **2002**.
[13] D. F. Evans, H. Wennerström, *The Colloidal Domain*, VCH Publishers, New York **1994**.
[14] J. N. Israelachvili, *Intermolecular and Surface Forces,* 2nd ed., Academic Press, Burlington **1991**.
[15] W. Stumm, J. J. Morgan, *Aquatic Chemistry*, Wiley-Interscience, New York **1996**.
[16] J. Widegren, L. Bergstrom, *J. Am. Ceram. Soc.* **2002**, *85*, 523–528.
[17] E. J. W. Verwey, J. T. G. Overbeek, *Theory of the Stability of Lyophobic Colloids*, Elsevier, Amsterdam **1948**.
[18] S. Ahn, E. C. Monge, S. C. Song, *Langmuir* **2009**, *25*, 2407–2418.
[19] *Carboxylic Acids. IUPAC Compendium of Chemical Terminology* (Eds: M. Nic, J. Jirat, B. Kosata), Online ed., **2006**.
[20] http://www.chemicalbook.com/ProductMSDSDetailCB6361837_EN.htm (accessed November 2012).
[21] G. B. Sukhorukov, A. A. Antipov, A. Voigt, E. Donath, H. Möhwald, *Macromol. Rapid Commun.* **2001**, *22*, 44–46.
[22] M. C. Beard, G. M. Turner, C. A. Schmuttenmaer, *Nano Lett.* **2002**, *2*, 983–987.
[23] K. H. Lee, R. Menon, C. O. Yoon, A. Heeger, *J. Phys. Rev. B* **1995**, *52*, 4779–4787.